厚生労働科学研究費補助金

食品の安全確保推進研究事業

短鎖および中鎖脂肪酸の腸管免疫修飾作用と安全性評価に関する研究

平成２５年度　総括分担研究報告書

研究代表者　長谷　耕二

平成２６（２０１４）年　５月

目　　次

Ⅰ．総括研究報告

短鎖および中鎖脂肪酸の腸管免疫修飾作用と安全性評価に関する研究　--- 1
長谷　耕二
（資料）図１および図２

II．分担研究報

１．食物アレルギーにおける短鎖および中鎖脂肪酸の安全性評価に関する研究 -5
國澤　純
（資料）資料名：図１－３

２．炎症性腸疾患患者における短鎖脂肪酸の解析に関する研究　---------- 9
飯島　英樹

III．研究成果の刊行に関する一覧表　---------- 11

IV．研究成果の刊行物･別刷　---------- 12

厚生労働科学研究費補助金（食品の安全確保推進研究事業）
（総括）研究報告書

短鎖および中鎖脂肪酸の腸管免疫修飾作用と安全性評価に関する研究

研究代表者　長谷　耕二　東京大学医科学研究所

研究要旨
腸内発酵の推進を目的としたプレバイオティクスと各種免疫疾患との関連については、これまで安全性評価の観点から十分に検証されていない。本研究では、炎症アレルギー性疾患との関連から、短鎖・中鎖脂肪酸の安全性について、基礎的・臨床的研究を遂行する。その結果、短鎖脂肪酸は大腸炎モデルに対する炎症抑制効果を示す一方で、食物アレルギーモデルにおける下痢を悪化させることが示唆された。中鎖脂肪酸に関しては特に炎症アレルギーへの効果は観察されなかった。病態モデルマウスで認められた知見をヒトにおいても確認するために、炎症性腸疾患患者の糞便サンプルの収集を開始した。

分担研究者:
國澤純（独立行政法人医薬基盤研究所・プロジェクトリーダー）
飯島英樹（大阪大学医学部・講師）

A. 研究目的

近年、「お腹の調子を整える」効果を謳った特定保健用食品が数多く普及しているが、これらは腸内細菌の発酵能を利用して短鎖脂肪酸など代謝物の産生を促すプレバイオティスクが主体である。短鎖脂肪酸はこれまで生体への有効性が強調されてきた。一方、腸管には多くの免疫担当細胞が存在しており、食品との不適切な免疫学的相互作用は、アレルギーや炎症などの発症を引き起こすことが判明している。つまり、食事性成分や発酵代謝産物には、腸管免疫応答の方向性を左右することで、各種免疫疾患の発症につながる潜在的な危険性が予想される。しかしながら、腸内発酵の推進を目的としたプレバイオティクスと各種免疫疾患との関連については、これまで安全性評価の観点から十分に検証されていない。同様に、体に脂肪がつきにくいことで食用油としての消費が高まっている中鎖脂肪酸についても、そのほとんどが健康への影響が懸念されている飽和脂肪酸であることから、免疫学的安全性を検証する必要がある。

そこで本研究では、炎症アレルギー性疾患との関連から、短鎖・中鎖脂肪酸の安全性について、基礎的・臨床的研究を遂行する。

B. 研究方法

マウス大腸炎モデルとして、CD45RBhi細胞移入誘発性大腸炎モデルおよび卵白アルブミン誘発性下痢モデル（国澤分担報告書参照）を用いた。大腸炎モデルでは、野生型マウスの脾臓よりCD3+CD4+CD45RBhi細胞をフローサイトメーターにより単離し、これをRag1欠損マウスに尾静脈注射した。その直後より短鎖脂肪酸脂肪酸を餌に混ぜて投与を行った。細胞移入後6週間に亘り、体重を測定した。6週目に病理組織学的解析を行った。

ヒト試料のうち炎症性腸疾患患者（クローン病、潰瘍性大腸炎）および健常者（各々30例）由来の糞便および大腸剖検サンプルは、研究分担者である飯島が採取中である（飯島

分担研究書参照)。

(倫理面への対応)

実験動物使用にあたっては、独立行政法人国立大学実験動物施設協議会指針に基づき、東京大学医科学研究所動物実験委員会の管理下で実験を行う(機関承認 PM25-61)。ヒトサンプルを用いた解析については、サンプルの収集を行う大阪大学医学系研究科、NTT 東日本関東病院、解析を行う東京大学医科学研究所、いずれにおいても倫理申請を終え承認を得ている[承認番号:13165 (大阪大学)、東総人医病企第 11-549 号 (NTT 東日本関東病院)、25-42-1122、および 21-36-1221(東大医科研)]

C. 研究結果

1) 炎症性腸疾患モデルにおける各種脂肪酸の影響

炎症性腸疾患では腸内細菌叢の異常がしばしば観察されることから、主要な腸内発酵代謝産物である短鎖脂肪酸(酢酸、プロピオン酸、酪酸) と病態との関わりが予想される。CD45RBhi 細胞移入により Rag1 欠損マウスに慢性大腸炎を誘導し (図1)、本モデルマウスに短鎖脂肪酸を食餌に混ぜて投与した。短鎖脂肪酸の投与により、盲腸および糞便中の短鎖脂肪酸濃度が上昇することを確認した。

本モデルでは大腸炎に伴う体重減少や大腸粘膜組織の肥厚が観察されるが、酪酸摂取群では、これらの症状が有意に抑制された(図2)。また制御性T細胞の割合が増加することが判明した。一方で、プロピオン酸や酢酸には大腸炎の抑制効果は認められなかった。これより、短鎖脂肪酸のうち酪酸は大腸炎に改善に有効であるとの結果が得られた。

2) 食物アレルギーモデルにおける各種脂肪酸の影響

本結果については分担研究報告書(国澤)を参照

3) 炎症性腸疾患患者糞便サンプルの取得

本結果については分担研究報告書(飯島)を参照

D. 考察

今回、酪酸による大腸炎の抑制作用が確認できた。酪酸は食物繊維の微生物発酵によって腸内で産生される。よって食物繊維含量が低く腸内発酵による酪酸産生が起こりにくい欧米型の食生活は炎症性腸疾患のリスクを高めると予想できる。今後、酪酸による炎症抑制メカニズムを調べるとともに、炎症性腸疾患患者と健常人から採取した糞便サンプルにおいて短鎖脂肪酸の濃度を測定する予定である。

E. 結論

酪酸には大腸炎を抑制する生理作用があることが判明した。食品の安全性を考慮した場合には、腸内発酵を初めとする腸内環境への食品の影響を十分に考慮する必要がある。

F. 健康危険情報

なし

G. 研究発表

1. 論文発表

① Furusawa Y, Obata Y, Fukuda S, Endo TA, Nakato G, Takahashi D, Nakanishi Y, Uetake C, Kato K, Kato T, Takahashi M, Fukuda NR, Murakami M, Miyauchi E, Hino S, Atarashi K, Onawa S, Fujimura Y, Lockett T, Clarke JM, Topping DL, Tomita M, Hori S, Ohara O, Morita T, Koseki H, Kikuchi J, Honda K, Hase K & Ohno H. Commensal microbe-derived butyrate induces colonic regulatory T cells. **Nature** 2013, **504**: 446-450, 2013.

2. 学会発表

① 長谷耕二, 腸内発酵産物による粘膜免疫修飾作用, 第67回栄養食糧学会大会, 2013年5月24-25日, 名古屋 (招待講演)

② Koji Hase, Commensal microbiota shapes the gut immune system through epigenetic modificaitons. The 8th RCAI-JSI International Symposium on Immunology 2013 (招待講演)

H．知的財産権の出願・登録状況

なし

図１大腸炎モデルマウスの作成

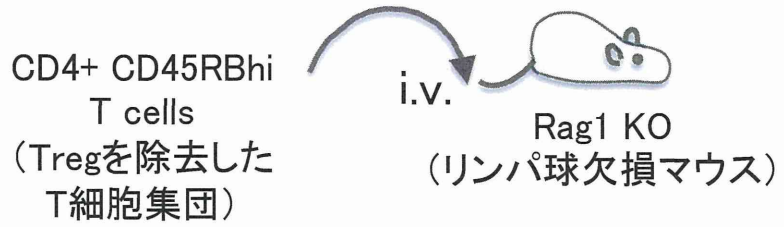

図２　大腸炎モデルにおける
体重変化(%)

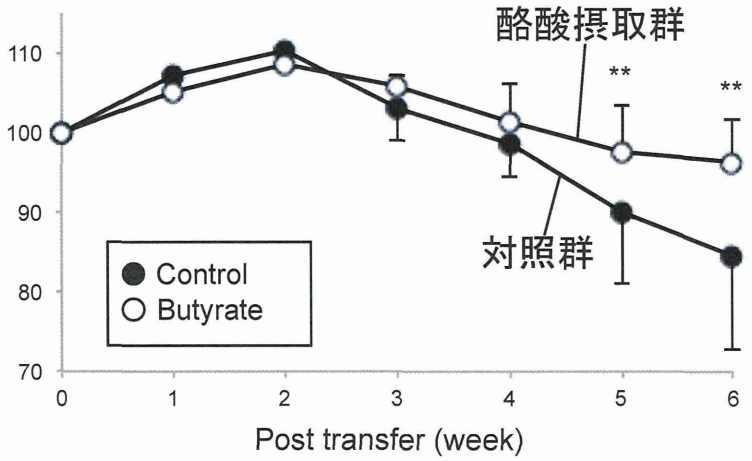

厚生労働科学研究費補助金（食品の安全確保推進　研究事業）
「短鎖および中鎖脂肪酸の腸管免疫修飾作用と安全性評価」
研究報告書

食物アレルギーにおける短鎖および中鎖脂肪酸の安全性評価に関する研究

研究分担者　國澤　純　　（独）医薬基盤研究所　　プロジェクトリーダー
研究協力者　長竹貴広　　同上　　研究員

研究要旨

近年、「お腹の調子を整える」「体に脂肪がつきにくい」などの効果を謳った特定保健用食品が数多く普及しているが、これらには腸内細菌の発酵能を利用して産生される短鎖脂肪酸やエネルギー変換効率の高い中鎖脂肪酸が主体となっているものが含まれる。一方でこれら機能性食品の作用を最も強くうけると考えられる腸管には多くの免疫担当細胞が存在しており、食品との不適切な免疫学的相互作用はアレルギーや炎症などの発症を引き起こすことが判明している。つまりこれまで有効性が強調されてきた機能性食品においても腸管免疫応答の方向性を左右することで、各種免疫疾患の発症につながる潜在的な危険性が考えられる。そこで本研究ではこれまであまり研究のすすんでいない短鎖および中鎖脂肪酸に着目し、食物アレルギーへの影響を解析している。本事業の初年度にあたるH25年度は短鎖脂肪酸に焦点を当てた解析を行い、短鎖脂肪酸の一つであるプロピオン酸が食物アレルギーモデルにおいて、アレルゲン特異的IgEの産生やマスト（肥満）細胞の脱顆粒に影響を与えることなく下痢症状を悪化させることを見いだした。

A. 研究目的

近年、「お腹の調子を整える」「体に脂肪がつきにくい」などの効果を謳った特定保健用食品が普及しているが、これらには腸内細菌の発酵能を利用して産生される短鎖脂肪酸やエネルギー変換効率の高い中鎖脂肪酸が主体となっているものが含まれる。これらは生体応答の一側面から有効性が強調されているが、腸管に多く存在し、生体の免疫応答や代謝などを制御している免疫担当細胞との相互作用については十分に解析されているとは言えないのが現状である。特に食品との不適切な免疫学的相互作用は、アレルギーや炎症などの発症を引き起こすことが判明していることを考えると、これら機能性食品により腸管免疫応答の方向性が規定されることで、各種免疫疾患の発症につながる潜在的な危険性が予想される。そこで本研究では、これまであまり研究のすすんでいない短鎖脂肪酸と中鎖脂肪酸に着目し、食物アレルギーへの影響を解析した。本事業の初年度にあたるH25年度は短鎖脂肪酸に焦点を当てた解析を行った。

B. 研究方法

でんぷんにプロピオン酸を結合させた特殊飼料を含む餌で1ヶ月飼育したマウスに、フロイント完全アジュバントを用い 1 mg の卵白アルブミン（OVA）を皮下投与することで全身感作を行った。全身感作の一週間後から週3回の頻度で50 mg の OVA を経口投与することでアレルギー性下痢を誘導し、下痢の発症を OVA 投与1時間後に観察した。

血清中のOVA特異的IgE抗体、ならびにmouse mast cell protease-1 (mMCP-1)の産生は DS mouse IgE ELISA (OVA) kit (DS ファーマ社)と mouse MCPT-1 (mMCP-1) ELISA kit (eBioscience 社)を用い、プロトコルに従い測定した。

(倫理面への配慮)
動物実験は(独)医薬基盤研究所のガイドラインに則り行った(承認番号 DS25-2R4)。

C. 研究結果

水溶性脂肪酸であり、腸内発酵によって生理的に産生される各種短鎖脂肪酸の食物アレルギーに対する安全性を評価したところ、大腸組織でプロピオン酸が大量に産生される特殊餌で飼育したマウスでは特にアレルギー誘導初期における顕著なアレルギー性下痢の増悪化が認められた(図1)。一方で別の短鎖脂肪酸である酢酸群では下痢発症に変化は認められなかった(データは示さず)。

本食物アレルギーモデルはIL-4などのTh2型サイトカインの産生、アレルゲン特異的IgE抗体の産生、マスト細胞の大腸への集積、マスト細胞の活性化と脱顆粒、といった免疫学的連続反応によりアレルギー性下痢が誘導されるI型アレルギーモデルである。そこでプロピオン酸による腸管アレルギー増悪化の作用点を解析する目的で、アレルギーの誘導と発症において重要因子となるアレルゲン特異的IgEの産生とマスト細胞の脱顆粒を測定した。その結果、プロピオン酸群ではアレルギー性下痢の発症促進が起こっているのにも関わらず、アレルゲン特異的IgE産生、マスト細胞脱顆粒マーカーmMCP-1の産生に変化は認められなかった(図2, 図3)。

D. 考察

短鎖脂肪酸は極めて類似した構造を取るにも関わらず、本食物アレルギーモデルにおいてはプロピオン酸において選択的なアレルギー性下痢の増悪化が認められた。短鎖脂肪酸の生理作用としてGpr41, Gpr43, Gpr109aなどの受容体を介した作用やヒストンアセチル化阻害作用が知られている。短鎖脂肪酸の鎖長により各受容体への結合性が変化することが知られていることから、短鎖脂肪酸間における各受容体の結合性、ならびに受容体を発現している細胞の検証が重要であると考える。

一方、免疫学的作用機序を検討したところ、アレルギー誘導因子であるアレルゲン特異的IgE 抗体の産生、さらにはアレルギー発症因子であるマスト細胞の脱顆粒に変化は認められなかった。このことからプロピオン酸はマスト細胞の脱顆粒以降のイベントである上皮細胞を介したイオンバランス・透過性制御機構に作用している可能性が考えられる。

E. 結論

プロピオン酸には食物アレルギーを悪化させる可能性が示唆されることから、プロピオン酸を増加させる食品については免疫学的な安全性を考慮する必要がある。

F. 健康危険情報

なし

G. 研究発表

1. 論文発表

1. A. Lamichhane, H. Kiyono, and J. Kunisawa*, Nutritional components regulate the gut immune system and its association with intestinal immune disease development, J Gastroenterol Hepatol 28: 18-24, 2013

2. J. Kunisawa* and H. Kiyono, Vitamin-mediated regulation of intestinal immunity. Front in Immunol 4:189, 2013

3. J. Kunisawa* and H. Kiyono, Immune regulation and surveillance at the

epithelial surface of the intestine. **Drug Discov Today** 18:87-92, 2013

4. S. Kishino, M. Takeuchia, S.B. Park, A. Hirata, N. Kitamura, J. Kunisawa, H. Kiyono, R. Iwamoto, Y. Isobe, M. Arita, H. Arai, K. Ueda, J. Shima, S. Takahashi, K. Yokozeki, S. Shimizu, and J. Ogawa, Novel fatty acid metabolism in gut lactic acid bacteria affecting host lipid composition, **Proc Natl Acad Sci USA** 110: 17808-17813, 2013

2. 学会発表

1. 國澤純　脂質ネットワークを介した腸管免疫の制御と創薬への展開　千里ライフセミナー　メタボローム研究の疾患への応用を目指して　大阪（千里ライフサイエンスセミナー）（2013年5月26日）（招待講演）

2. 國澤純　腸内環境ネットワークによる免疫制御とワクチン開発、創薬への展開　第12回四国免疫フォーラム　香川（徳島文理大学香川校（2013年6月22日）（招待講演）

3. 國澤純　腸内フローラと腸管免疫による疾患制御　第13回日本抗加齢医学会総会　横浜（パシフィコ横浜）（2013年6月28日）（招待講演）

4. 國澤純　腸内環境を介した免疫制御と炎症性腸疾患　第34回日本炎症・再生医学会　京都（国立京都国際会館）（2013年7月2日）（招待講演）

5. 國澤純　腸管免疫ネットワークを標的とした創薬研究の最前線　第5回生命科学阿波おどりシンポジウム　徳島（徳島大学）（2013年8月16日）（招待講演）

6. 國澤純、腸内環境因子を介した免疫制御と疾患、創薬・ワクチンへの展開　第9回霊長類医科学フォーラム　つくば（文部科学省研究交流センター）（2013年11月14日）（招待講演）

H．知的財産権の出願・登録状況

なし

図1 プロピオン酸含有餌で飼育したマウスでは
食物アレルギーモデルで誘導される下痢症状が
増悪化する

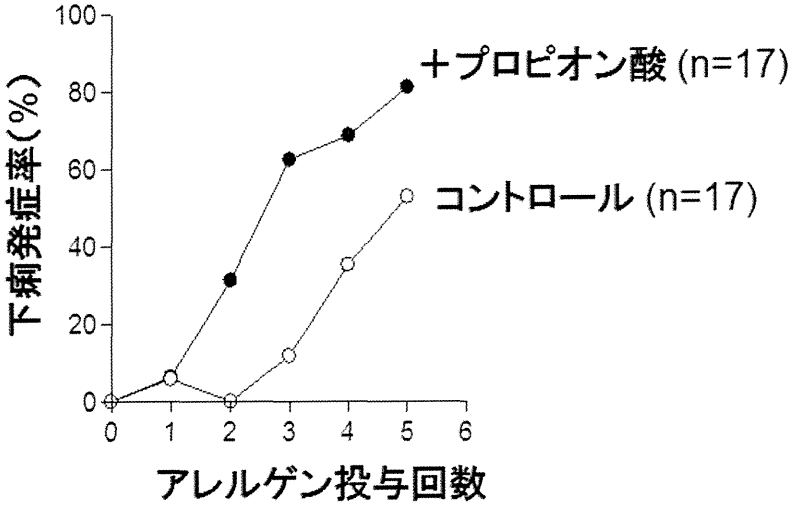

図2 アレルギー性下痢誘導時に
おけるアレルゲン特異的IgEの産生

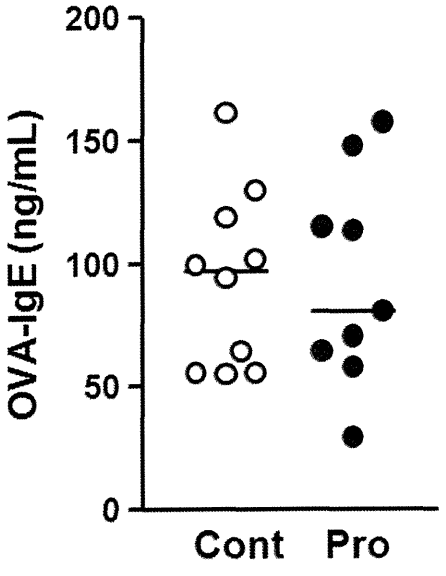

Cont: コントロール
Pro: プロピオン酸

図3 アレルギー性下痢誘導時に
おけるマスト細胞脱顆粒マーカー
(mMCP-1)の産生

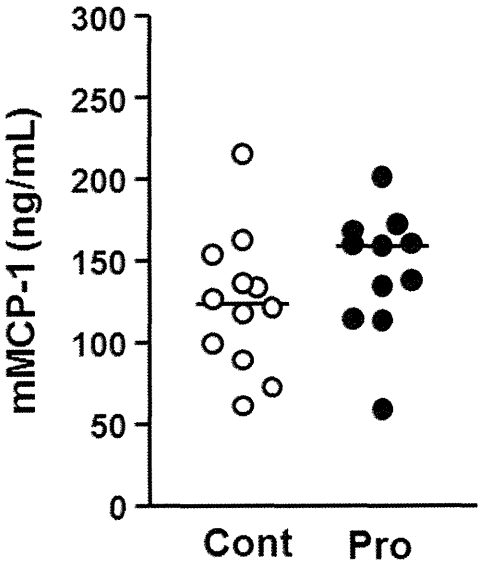

Cont: コントロール
Pro: プロピオン酸

厚生労働科学研究費補助金（食品の安全確保推進　研究事業）
「短鎖および中鎖脂肪酸の腸管免疫修飾作用と安全性評価」
研究報告書

炎症性腸疾患患者における短鎖脂肪酸の解析に関する研究

研究分担者　飯島　英樹　大阪大学医学部　講師

研究要旨

近年、「お腹の調子を整える」「体に脂肪がつきにくい」などの効果を謳った特定保健用食品が数多く普及しているが、これらには腸内細菌の発酵能を利用して産生される短鎖脂肪酸やエネルギー変換効率の高い中鎖脂肪酸が主体となっているものが含まれる。一方でこれら機能性食品の作用を最も強くうけると考えられる腸管には多くの免疫担当細胞が存在しており、食品との不適切な免疫学的相互作用はアレルギーや炎症などの発症を引き起こすことが判明している。つまりこれまで有効性が強調されてきた機能性食品においても腸管免疫応答の方向性を左右することで、各種免疫疾患の発症につながる潜在的な危険性が考えられる。そこで本研究ではこれまであまり研究のすすんでいない短鎖および中鎖脂肪酸に着目し、食物アレルギーへの影響を解析している。本事業の初年度にあたるH25年度は短鎖脂肪酸に焦点を当てた解析を行い、炎症性腸疾患患者の糞便サンプルにおける短鎖脂肪酸濃度を測定するための試料の採取を行った。

A. 研究目的

短鎖脂肪酸は腸管生理や脂質代謝に様々な影響を及ぼすことが報告されている。一方で免疫系への影響については不明な点が多い。腸管には多くの免疫担当細胞が存在しており、食品との不適切な免疫学的相互作用は、アレルギーや炎症などの発症を引き起こすことが判明している。つまり、食事性成分や発酵代謝産物には、腸管免疫応答の方向性を左右することで、各種免疫疾患の発症につながる潜在的な危険性が予想される。本研究は、炎症性腸疾患患者の糞便サンプルにおける短鎖脂肪酸濃度を測定することで、疾患発症との関わりを解析する。

B. 研究方法

大阪大学医学部附属病院に通院中の潰瘍性大腸炎患者、クローン病患者および健常ボランティアより糞便約20ｇの提供を受け、速やかに匿名化の上-80度に保存する。検体は、大阪大学消化器内科、東京大学医科学研究所・国際粘膜ワクチンセンター　粘膜バリア学、独立行政法人　医薬基盤研究所　ワクチンマテリアルプロジェクト、静岡大学農学部・応用生物化学科　食品栄養化学研究室にて成分の解析を行う。

（倫理面への配慮）

本研究は、事前に大阪大学医学系研究科における倫理申請を終え承認を得て実施している[承認番号：13165（大阪大学）]。

C. 研究結果

健常人および炎症性腸疾患（潰瘍性大腸炎またはクローン病）患者との間で糞便および血液中の短鎖脂肪酸濃度に関する基礎データを取得するため、倫理委員会への申請を行い、承認が得られたためサンプルの収集を開始した。同様に小児アレルギー疾患と脂肪酸の関わりを調べるために、糞便に含まれる脂肪酸の基礎データを取得するための倫理申請を行い、承認を得て

サンプリングを開始している。サンプルが揃い次第、短鎖脂肪酸の解析を実施する。

D．考察

現在サンプリング中のため省略。

E．結論

現在サンプリング中のため省略。

F．健康危険情報

なし

G．研究発表

1. 論文発表

なし

2. 学会発表

なし

H．知的財産権の出願・登録状況

なし

III. 研究成果の刊行に関する一覧表

雑誌

発表者氏名	論文タイトル名	発表誌名	巻号	ページ	出版年
Furusawa Y, Obata Y, Fukuda S, Endo TA, Nakato G, Takahashi D, Nakanishi Y, Uetake C, Kato K, Kato T, Takahashi M, Fukuda NR, Murakami M, Miyauchi E, Hino S, Atarashi K, Onawa S, Fujimura Y, Lockett T, Clarke JM, Topping DL, Tomita M, Hori S, Ohara O, Morita T, Koseki H, Kikuchi J, Honda K, Hase K & Ohno H.	Commensal microbe-derived butyrate induces colonic regulatory T cells.	Nature	504	446-450	2013
A. Lamichhane, H. Kiyono, and J. Kunisawa	Nutritional components regulate the gut immune system and its association with intestinal immune disease development,	J Gastroenterol Hepatol	28	18-24	2013
J. Kunisawa and H. Kiyono,	Vitamin-mediated regulation of intestinal immunity	Front in Immunol	4	189	2013
J. Kunisawa and H. Kiyono,	Immune regulation and surveillance at the epithelial surface of the intestine.	Drug Discov Today	18	87-92	2013
S. Kishino, M. Takeuchia, S. B. Park, A. Hirata, N. Kitamura, J. Kunisawa, H. Kiyono, R. Iwamoto, Y. Isobe, M. Arita, H. Arai, K. Ueda, J. Shima, S. Takahashi, K. Yokozeki, S. Shimizu, and J. Ogawa	Novel fatty acid metabolism in gut lactic acid bacteria affecting host lipid composition,	Proc Natl Acad Sci USA	110	17808-17813	2013

III. 研究成果の刊行物・別刷り

LETTER

doi:10.1038/nature12721

Commensal microbe-derived butyrate induces the differentiation of colonic regulatory T cells

Yukihiro Furusawa[1,2]*, Yuuki Obata[1,2,3]*, Shinji Fukuda[1,4]*, Takaho A. Endo[1], Gaku Nakato[1], Daisuke Takahashi[1], Yumiko Nakanishi[4], Chikako Uetake[1], Keiko Kato[1,5], Tamotsu Kato[1], Masumi Takahashi[1], Noriko N. Fukuda[4], Shinnosuke Murakami[4], Eiji Miyauchi[1], Shingo Hino[6], Koji Atarashi[1,7], Satoshi Onawa[1], Yumiko Fujimura[2], Trevor Lockett[8], Julie M. Clarke[8], David L. Topping[8], Masaru Tomita[4], Shohei Hori[1], Osamu Ohara[1], Tatsuya Morita[6], Haruhiko Koseki[1,3,5], Jun Kikuchi[5,9], Kenya Honda[1,10], Koji Hase[1,2,7]* & Hiroshi Ohno[1,3,5]

Gut commensal microbes shape the mucosal immune system by regulating the differentiation and expansion of several types of T cell[1–5]. *Clostridia*, a dominant class of commensal microbe, can induce colonic regulatory T (T_{reg}) cells, which have a central role in the suppression of inflammatory and allergic responses[3]. However, the molecular mechanisms by which commensal microbes induce colonic T_{reg} cells have been unclear. Here we show that a large bowel microbial fermentation product, butyrate, induces the differentiation of colonic T_{reg} cells in mice. A comparative NMR-based metabolome analysis suggests that the luminal concentrations of short-chain fatty acids positively correlates with the number of T_{reg} cells in the colon. Among short-chain fatty acids, butyrate induced the differentiation of T_{reg} cells *in vitro* and *in vivo*, and ameliorated the development of colitis induced by adoptive transfer of $CD4^+$ $CD45RB^{hi}$ T cells in *Rag1*$^{-/-}$ mice. Treatment of naive T cells under the T_{reg}-cell-polarizing conditions with butyrate enhanced histone H3 acetylation in the promoter and conserved non-coding sequence regions of the *Foxp3* locus, suggesting a possible mechanism for how microbial-derived butyrate regulates the differentiation of T_{reg} cells. Our findings provide new insight into the mechanisms by which host–microbe interactions establish immunological homeostasis in the gut.

Germ-free mice have an enlarged caecum because of the accumulation of hydrated dietary fibre components. Colonization with chloroform-resistant bacteria (CRB)[6] normalizes caecal size, probably through fermentation of these components by the CRB (Fig. 1a, b). Therefore, CRB-derived dietary fibre metabolites could be responsible for the induction of colonic T_{reg} cells. To assess this possibility, CRB-associated mice were fed either a low-fibre diet (LFD) or a high-fibre diet (HFD). In CRB-associated HFD-fed (CRB-HFD) mice, the expression of neuropilin-1^- and $Helios^-$ (also known as $IKZF2^-$) T_{reg} cells, which represent the peripherally generated T_{reg} cell population[7–9], was significantly increased (Fig. 1c, d and Supplementary Figs 1 and 2). Consistent with previous observations[3], the effect of CRB on T_{reg} cell induction was restricted to the colon and not the mesenteric lymph nodes or spleen (Supplementary Fig. 3). In addition, the expression of $CD103^+$-activated T_{reg} cells was also increased in CRB-HFD mice (Fig. 1d). Notably, a LFD compromised the effects of CRB colonization on T_{reg} cell induction (Fig. 1c, d), despite the comparable number and composition of gut microbes predominantly annotated as *Clostridiales* (Supplementary Figs 4–6). These observations strongly suggest that metabolic differences in gut microbes are responsible for the differential T_{reg} cell inducibility between CRB-HFD and CRB-LFD mice.

Indeed, principal component analysis (PCA) and orthogonal partial least squares discriminate analysis of the NMR-based metabolome data

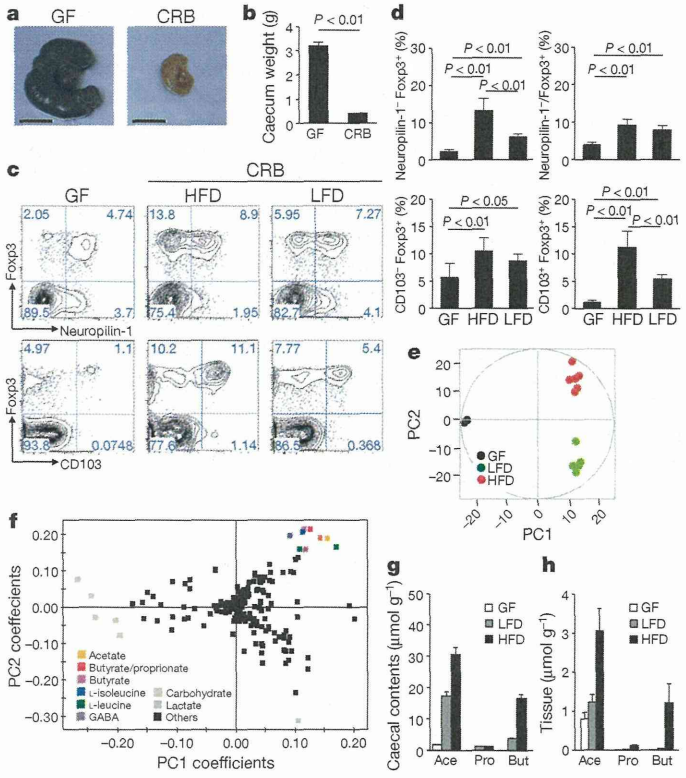

Figure 1 | Gut microbial metabolism is essential for the induction of colonic T_{reg} cells. **a**, **b**, The caecum size of germ-free (GF) and CRB-associated mice. Representative caecum images are shown in **a**. Scale bars, 1 cm. **c**, **d**, The expression of neuropilin-1 and CD103 in $Foxp3^+$ T cells in germ-free and CRB-associated mice fed a HFD or LFD for 4 weeks. Representative FACS plots gated on $CD3^{\varepsilon+}$ $CD4^+$ are shown in **c**. *P* value was determined by one-way analysis of variance (ANOVA) followed by Tukey's post-hoc test. **e**, **f**, Caecal metabolomic profiling by NMR of germ-free and CRB mice fed a HFD or LFD. The results of PCA on the ^{1}H-NMR data (**e**) and loading scatter plot (**f**) are shown. Proportions of the first (PC1) and second (PC2) principal components are 85.1% and 10.3%, respectively. The ellipse denotes the 95% significance limit of the model, as defined by Hotelling's *t*-test. **g**, **h**, Organic acids in caecal contents (**g**) and the proximal colonic tissue (**h**) were measured by gas chromatography–mass spectrometry. Ace, acetate; but, butyrate; pro, propionate. Error bars indicate s.e.m. (**b**, $n = 5$) or s.d. (**d**, $n = 10$; **g**, **h**, $n = 7$). All data are representative of two (**e**–**h**) or three (**a**–**d**) independent experiments.

[1]RIKEN Center for Integrative Medical Sciences (IMS-RCAI), Kanagawa 230-0045, Japan. [2]The Institute of Medical Science, The University of Tokyo, Tokyo 108-8639, Japan. [3]Graduate School of Medicine, Chiba University, Chiba 260-8670, Japan. [4]Institute for Advanced Biosciences, Keio University, Yamagata 997-0052, Japan. [5]Graduate School of Medical Life Science, Yokohama City University, Kanagawa 230-0045, Japan. [6]Faculty of Agriculture, Shizuoka University, Shizuoka 422-8529, Japan. [7]PRESTO, Japan Science and Technology Agency, Saitama 332-0012, Japan. [8]Preventative Health National Research Flagship, CSIRO Food and Nutritional Sciences, South Australia 5000, Australia. [9]RIKEN Center for Sustainable Resource Science, Kanagawa 230-0045, Japan. [10]CREST, Japan Science and Technology Agency, Saitama 332-0012, Japan.
*These authors contributed equally to this work.

indicated that the amount of caecal short-chain fatty acids (SCFAs), namely acetate, propionate and butyrate, was higher in CRB-HFD than in CRB-LFD mice (Fig. 1e, f, Supplementary Fig. 7 and Supplementary Table 1). Quantitative analysis confirmed a significant increase in acetate and butyrate in the caecal content and colonic tissues of CRB-HFD mice (Fig. 1g, h). Luminal GABA (γ-aminobutyric acid), L-leucine and L-isoleucine were also increased in CRB-HFD mice (Fig. 1f and Supplementary Fig. 7). To test whether these metabolites can induce T_{reg} cells *in vitro*, splenic naive ($CD44^{lo}$ $CD62L^{hi}$) $CD4^+$ T cells were cultured in the presence of T-cell antigen receptor and CD28 signalling plus TGF-β with or without each metabolite. Butyrate significantly increased the frequency of $Foxp3^+$ cells (Fig. 2a, b). Propionate showed a moderate effect, whereas the other metabolites, including acetate, did not have any effect on T_{reg} cell induction at physiological concentrations (Fig. 2a, b and Supplementary Fig. 8).

To corroborate the role of butyrate in T_{reg} cell induction *in vivo*, specific pathogen-free (SPF) C57BL/6 mice were fed modified diets containing acetylated, propionylated or butyrylated high-amylose maize starches[10] (HAMSA, HAMSP or HAMSB, respectively) to increase the luminal levels of the corresponding SCFA (Fig. 2c). Consistent with the *in vitro* observations, colonic T_{reg} cells were significantly augmented when the diet contained HAMSB, whereas HAMSP slightly and HAMSA barely induced T_{reg} cells in SPF mice (Fig. 2d, e and Supplementary Fig. 9). The HAMSB diet also increased the number of ovalbumin (OVA)-specific colonic OT-II $Foxp3^+$ cells from adoptively transferred OT-II naive $CD4^+$ T cells (Fig. 2f, g). Because butyrate did not affect the survival or the proliferation of colonic T_{reg} cells (Supplementary Figs 10 and 11), this increase probably reflects a role for this SCFA in regulating T_{reg} cell differentiation. Furthermore, the intake of HAMSB increased colonic T_{reg} cells in germ-free mice mono-associated with *Bacteroides thetaiotaomicron*, an organism devoid of butyrate-producing and T_{reg}-cell-inducing activities per se[3] (Supplementary Fig. 12). Under germ-free conditions, HAMSB did not increase T_{reg} cells, suggesting that the presence of commensal bacteria is a prerequisite for T_{reg} cell induction (Supplementary Fig. 13).

Interleukin (IL)-10 production by T_{reg} cells is well documented to be required for containment of inflammatory responses in mucosal tissues including the colon[11], and the colonization with a mixture of *Clostridiales* is sufficient to induce IL-10-producing T_{reg} cells[3]. Likewise, the intake of HAMSB significantly increased IL-10-producing T_{reg} cells in the colon (Fig. 2h). Collectively, these observations illustrate that butyrate has a key role in the commensal-microbe-mediated differentiation of functional T_{reg} cells in the colon.

We also explored the effect of butyrate on the differentiation of naive T cells into other $CD4^+$ T-cell subsets. Treatment with butyrate or feeding of HAMSB did not affect the induction of T-bet, GATA3 and RORγt, the master regulators of T helper 1 (T_H1), T_H2 and T_H17 cells, respectively (Supplementary Figs 14 and 15). Notably, butyrate promoted the induction of $Foxp3^+$ cells even under T_H1- and T_H17-polarizing conditions. These data strongly suggest that butyrate preferentially induces T_{reg} cell differentiation.

The requirement for the Toll-like receptor (TLR)–MyD88 signalling pathway[12] in commensal microbe-induced T_{reg} cell expansion seems to be variable depending on the type of bacteria involved[3–5,13]. We observed that treatment of SPF *Myd88*$^{-/-}$ *Ticam1*$^{-/-}$ mice with HAMSB induced colonic T_{reg} cells (Supplementary Fig. 16) to the same extent as in wild-type mice (Fig. 2d, e). Therefore, TLR–MyD88 signalling is dispensable for butyrate-dependent T_{reg} cell induction in the colon.

Butyrate is well known to regulate gene expression epigenetically by inhibiting histone deacetylases (HDACs)[14,15], specifically classes IIa and I of the four HDAC classes identified in mammals. Because class IIa HDAC has been reported to suppress T_{reg} cell expansion[16,17], butyrate may influence histone acetylation of gut $CD4^+$ T cells to regulate epigenetically the transcription of the genes responsible for T_{reg} cell induction. To verify this hypothesis, we performed chromatin immunoprecipitation sequencing (ChIP-seq) analysis of naive $CD4^+$ T cells treated with or without butyrate under T_{reg}-cell-polarizing conditions. Butyrate slightly increased genome-wide histone H3 acetylation (Supplementary Fig. 17). Consistently, the histone acetylation status of the promoter regions of most transcription factors was unchanged

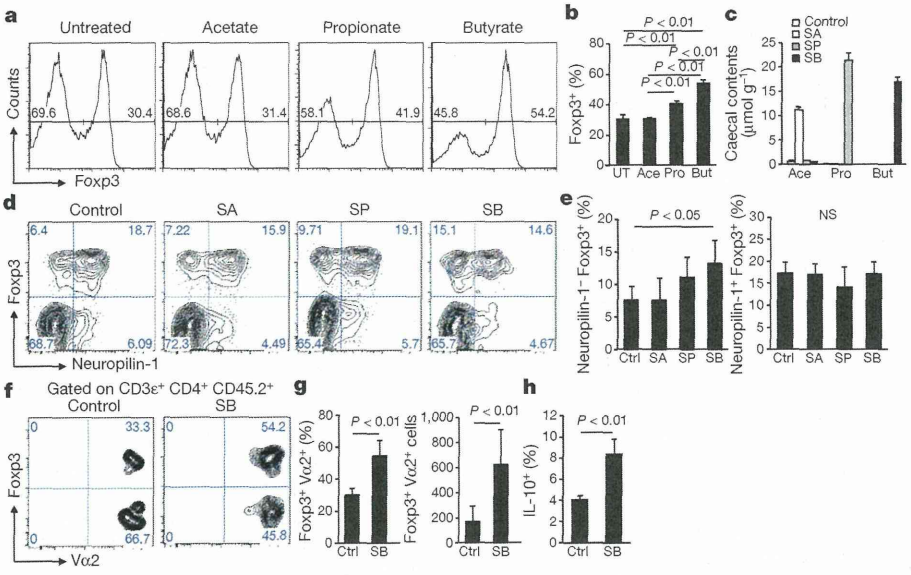

Figure 2 | Butyrate induces the differentiation of T_{reg} cells in the colonic lamina propria. **a**, **b**, Naive $CD4^+$ T cells were stimulated with immobilized anti-CD3 and soluble anti-CD28 monoclonal antibodies in the absence (untreated; UT) or presence of acetate, propionate or butyrate. Representative FACS plots are shown in **a**. **c**, Amount of caecal SCFA in the mice fed with control HAMS diet or diets containing HAMSA, HAMSP or HAMSB (SA, SP or SB, respectively). **d**, **e**, FACS profile of colonic lamina propria cells. The representative FACS plots gated on $CD3\varepsilon^+$ $CD4^+$ cells are shown in **d**. **e**, The frequency of neuropilin-1^- and neuropilin-1^+ $Foxp3^+$ cells among $CD4^+$ T cells. **f**, **g**, The percentage and total number of OVA-induced $Foxp3^+$ cells in mice fed with HAMS control (Ctrl) or HAMSB (SB). Representative FACS plots gated on $CD3\varepsilon^+$ $CD4^+$ $CD45.2^+$ are shown in **f**. $CD45.2^+$ $V\alpha2^+$ $CD4^+$ T cells were sorted and adoptively transferred into $CD45.1^+$ C57BL/6 recipients, followed by administration of drinking water containing 1% ovalbumin (OVA) for 9 days before analysis. **h**, Percentage of IL-10^+ cells among $CD25^+$ $FR4^+$ colonic T_{reg} cells in SPF C57BL/6 mice fed with HAMS or HAMSB. Error bars indicate s.d. (**b**, $n = 3$; **c**, $n = 4$; **e**, $n = 5$; **g**, $n = 4$ for control and $n = 5$ for SB; **h**, $n = 5$). *P* values determined by non-parametrical Mann–Whitney *U* test (**g**, **h**) or one-way ANOVA followed by Tukey's post-hoc test (**b**, **e**). All data are representative of at least two independent experiments. NS, not significant.

or moderately upregulated (Fig. 3a–c), and only 70 transcription factors (4.73% of the genes categorized as a transcription factor), including *Foxp3*, were highly acetylated after butyrate exposure (Fig. 3b, pink area). Importantly, this increased histone acetylation was positively correlated with gene expression (Fig. 3c). *Foxp3* expression is regulated not only by its promoter but also by intragenic enhancer elements termed conserved noncoding sequence (CNS) 1–3 (ref. 18). Butyrate upregulated histone H3 acetylation at both the promoter and CNS3 of the *Foxp3* gene locus 1 day before *Foxp3* induction (Fig. 3a, d). Furthermore, butyrate exposure gradually increased the acetylated histone H3 status of the CNS1 region over the course of T_{reg} cell differentiation. In sharp contrast, no such epigenetic modifications were observed in the *Tbx21*, *Gata3* and *Rorc* genes after butyrate exposure (Supplementary Fig. 18). CNS1, which contains binding motifs for Smad3, NFAT and retinoic acid receptor, is important for the peripheral induction of *Foxp3* (ref. 18). Conversely, CNS3 contains a c-Rel binding motif, which establishes the *Foxp3*-specific enhanceosome and thus greatly enhances the probability of Foxp3 induction[19,20]. We detected little, if any, increase in histone H3 acetylation at the c-Rel, NFAT, Smad3 or Stat5 promoters after butyrate exposure (Supplementary Fig. 19). Correspondingly, expression levels of these genes remained unchanged (Supplementary Fig. 20). On the basis of these observations, we propose that butyrate probably augments the accessibility of these transcriptional regulators to the enhancer elements as well as the promoter region through acetylation of the *Foxp3* gene locus.

Finally, we investigated the function of the butyrate-induced T_{reg} cells in chronic intestinal inflammation by adoptively transferring $CD4^+$ $CD45RB^{hi}$ naive T cells into *Rag1*$^{-/-}$ mice[21]. Over the course of the

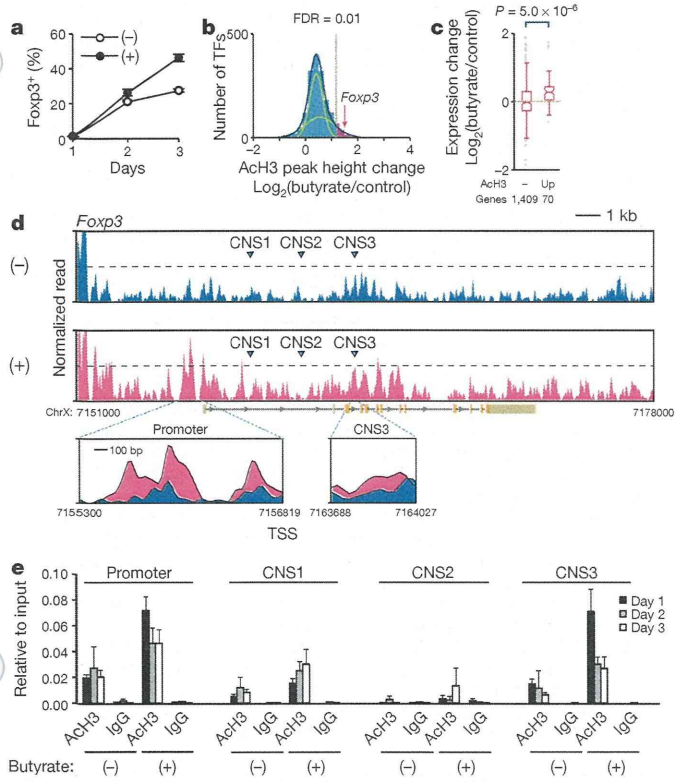

Figure 3 | Chromatin modification at the Foxp3 locus by butyrate. **a**, Time-course analysis on the differentiation of naive T cells into $Foxp3^+$ T_{reg} cells. Naive $CD4^+$ T cells were cultured under T_{reg}-cell-inducing condition in the absence (−) or presence (+) of butyrate. **b**–**d**, Acetylated histone H3 (AcH3) status of transcriptional regulator genes at day 1 after butyrate exposure was determined by ChIP-seq analysis. Distribution of acetylation changes in the gene loci encoding transcription factors (TFs) was fitted using multiple Gaussian distributions with the expectation–maximization algorithm (**b**). Using this analysis, we identified two groups representing upper (highly acetylated) and lower (moderately or not acetylated) transcriptional regulator genes after butyrate treatment. The threshold was set so that the false discovery ratio (FDR) in the upper group was 0.01, where 99% of transcriptional regulators with a high acetylation changes belonged to the upper group (**b**, pink area). Correlation of gene expression changes and the acetylated H3 status in transcriptional regulators is shown in **c**. Gene expression was analysed by microarray at day 2. The normalized number of sequence tags of DNA at the *Foxp3* promoter and gene body is shown in **d**. ChrX, chromosome X. **e**, ChIP quantitative PCR (qPCR) analysis of the *Foxp3* promoter and enhancer regions was performed in $CD4^+$ T cells cultured in the presence or absence of butyrate, using anti-AcH3 antibody or rabbit IgG as a negative control. Error bars indicate s.d (**a**, **e**, $n = 3$).

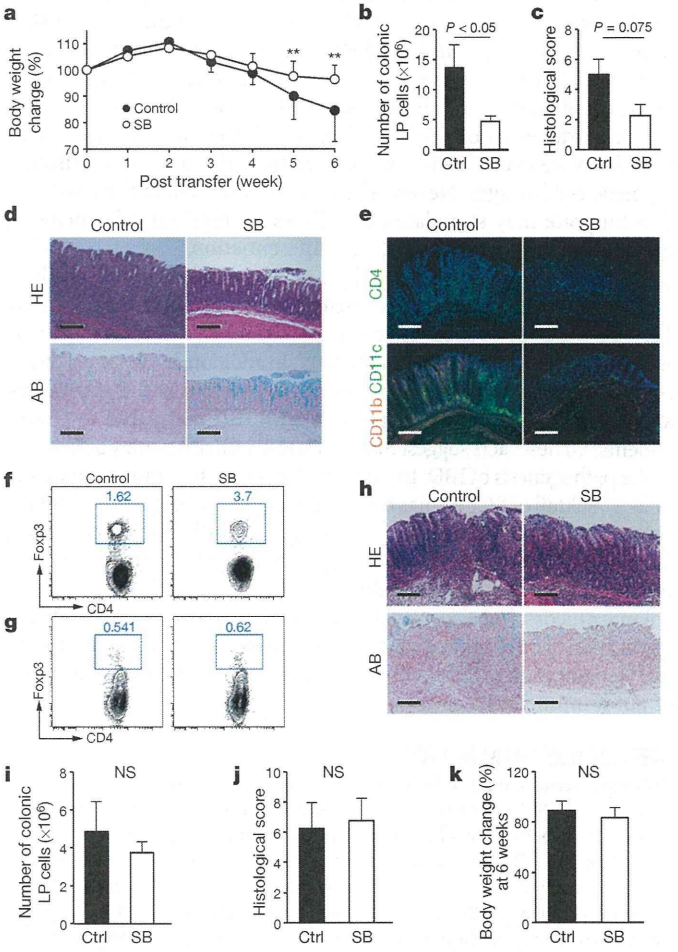

Figure 4 | Butyrate ameliorates T-cell-dependent experimental colitis. **a**–**f**, Experimental colitis was induced by adoptive transfer of $CD4^+$ $CD45RB^{hi}$ T cells in *Rag1*$^{-/-}$ mice fed with HAMS or HAMSB. **a**, Body weight change was monitored. **b**–**f**, The number of colonic lamina propria (LP)-infiltrating mononuclear cells (**b**) and histological score (**c**), representative colonic specimens stained with haematoxylin and eosin (HE) and Alcian blue (AB) (**d**), representative immunofluorescent staining images for CD4, CD11b, CD11c and nuclei (blue) (**e**) and the frequency of $Foxp3^+$ cells in the colonic mucosa (**f**) were analysed at 6 weeks after the cell transfer. **g**–**k**, $CD4^+$ $CD45RB^{hi}$ T cells from *Foxp3*^{hCD2} reporter mice were transferred into *Rag1*$^{-/-}$ recipients, which were injected intravenously with anti-human CD2 monoclonal antibody twice at 4 and 5 weeks after the cell transfer. Depletion of $Foxp3^+$ cells in the colonic lamina propria was confirmed by FACS analysis (**g**). The mice were analysed for colitis development at 6 weeks after transfer (**h**–**k**). Turquoise blue represents goblet cells (**d**, **h**, bottom). Error bars indicate s.d. (**a**, **b**, **c**, **f**, $n = 5$; **i**–**k**, $n = 4$). *P* values were determined by two-way repeated measures ANOVA followed by Tukey's test (**a**) and non-parametrical Mann–Whitney *U* test (**b**, **c**, **i**–**k**). $^{**}P < 0.01$ (**a**). Scale bars, 200 μm (**d**, **e**, **h**). All data are representative of two independent experiments.

experiment, the recipient mice were fed either a control HAMS- or a HAMSB-containing diet. The HAMS-fed group developed wasting disease in association with severe colitis. However, the intake of HAMSB, but not HAMSA or HAMSP, ameliorated the colitis development (Fig. 4a–f and Supplementary Fig. 21). This beneficial effect is at least partly attributed to the induction of colonic T_{reg} cells by butyrate. In support of this notion, depletion of T_{reg} cells abrogated the protective effect of HAMSB (Fig. 4g–k).

The present study demonstrates that butyrate produced by gut microbes induces functional colonic T_{reg} cells, specifically among $CD4^+$ T-cell subsets, via T-cell intrinsic epigenetic upregulation of the *Foxp3* gene. However, we do not formally exclude the possibility that effects of butyrate other than histone acetylation status, or targets of HDAC other than histones, may also be involved in T_{reg} cell differentiation. SCFAs have also been reported to act through cell surface signalling receptors such as G-protein-coupled receptor 43 (GPR43) to execute some of their functions[22]; however, this is unlikely to be the case for the effect of butyrate on T_{reg} cells, because acetate, which is a potent GPR43 ligand[23], failed to ameliorate T-cell-dependent experimental colitis or induce T_{reg} cell differentiation (Fig. 2a–e and Supplementary Fig. 21). In addition, the expression of GPR43 is restricted to myeloid cells among haematopoietic cell lineages. Nevertheless, we do not exclude the possibility that butyrate may stimulate other GPRs on myeloid cells including dendritic cells to facilitate T_{reg} cell differentiation.

Butyrate has been appreciated for its beneficial effects on the host, including trophic and anti-inflammatory effects on epithelial cells[24]. The butyrate transporter is downregulated in the colonic mucosa of patients with inflammatory bowel diseases (IBD)[25]. In addition, butyrate-producing bacteria are decreased in the intestinal microbiota at the gut mucosa and in the faecal samples of patients with IBD compared to control patients[26]. These facts suggest that butyrate insufficiency may be involved in the pathogenesis of IBD. In support of this idea, butyrate enema, alone or as a cocktail of SCFAs, has been shown to ameliorate colonic inflammation in patient with IBD[27,28], although the underlying mechanisms were not fully understood. Our findings not only link butyrate to commensal microbe-mediated induction of functional T_{reg} cells in the colonic mucosa, but also provide molecular insight into the therapeutic application of butyrate and how a metabolite produced by colonic microbial fermentation mediates host–microbial crosstalk for establishment of gut immune homeostasis (Supplementary Fig. 22).

METHODS SUMMARY

Animals. Germ-free IQI mice were housed in germ-free isolators in the animal facility of RIKEN. Eight-to-ten-week-old male or female germ-free mice were orally inoculated with 3% (v/v) chloroform-treated murine faecal suspension (CRB)[6]. Germ-free and CRB-associated mice, which were housed in different isolators, were randomly grouped, and each group was fed with a γ-ray-sterilized CMF chow (Oriental Yeast) as a HFD, or AIN93G-fomula diet (Oriental Yeast) as a LFD for 4 weeks. To generate *B.-thetaiotaomicron*-associated mice, male or female germ-free mice of 8–16 weeks of age were colonized with a single gavage of 10^8 colony-forming units of *B. thetaiotaomicron*, JCM 5827T (Japan Collection of Microorganisms). Ten days after the inoculation, *B.-thetaiotaomicron*-associated mice were randomly grouped and each group was fed with the diet containing 15% (w/w) HAMS and HAMSB as a substitute for corn starch for 4 weeks. C57BL/6 mice and *Myd88*$^{-/-}$*Ticam1*$^{-/-}$ mice were purchased from CLEA Japan and Oriental Bioservice, respectively. Mice were fed with AIN93G as a control diet for a week, and subsequently a diet containing 15% (w/w) HAMS, HAMSA, HAMSP or HAMSB for 4 weeks. *Foxp3-hCD2-hCD52* knock-in (*Foxp3*^{hCD2}) mice were described previously[29]. OT-II transgenic mice were from the Jackson Laboratory. All animal experiments were performed using protocols approved by Animal Studies Committees of RIKEN Yokohama Institute and Yokohama City University. Sample size was determined based on published studies using similar assays as well as the previous experience of the senior authors. No blinding was done for animal studies.

Adoptive transfer of OT-II T cells. OT-II (Ly5.2) transgenic $CD4^+$ T cells were enriched from the spleen and lymph nodes using the IMag Cell Separation System. $CD3^+$ $CD4^+$ $CD25^-$ $V\alpha2^+$ cells were sorted using FACSAriaII and intravenously transferred into C57BL/6 (Ly5.1) mice. Recipient mice were administered 1% ovalbumin in drinking water for 9 days.

Online Content Any additional Methods, Extended Data display items and Source Data are available in the online version of the paper; references unique to these sections appear only in the online paper.

Received 18 June; accepted 27 September 2013.
Published online 13 November 2013.

1. Chung, H. *et al.* Gut immune maturation depends on colonization with a host-specific microbiota. *Cell* **149,** 1578–1593 (2012).
2. Ivanov, I. I. *et al.* Induction of intestinal Th17 cells by segmented filamentous bacteria. *Cell* **139,** 485–498 (2009).
3. Atarashi, K. *et al.* Induction of colonic regulatory T cells by indigenous clostridium species. *Science* **331,** 337–341 (2011).
4. Geuking, M. B. *et al.* Intestinal bacterial colonization induces mutualistic regulatory T cell responses. *Immunity* **34,** 794–806 (2011).
5. Round, J. L. & Mazmanian, S. K. Inducible $Foxp3^+$ regulatory T-cell development by a commensal bacterium of the intestinal microbiota. *Proc. Natl Acad. Sci. USA* **107,** 12204–12209 (2010).
6. Itoh, K. & Mitsuoka, T. Characterization of clostridia isolated from faeces of limited flora mice and their effect on caecal size when associated with germ-free mice. *Lab. Anim.* **19,** 111–118 (1985).
7. Thornton, A. M. *et al.* Expression of Helios, an Ikaros transcription factor family member, differentiates thymic-derived from peripherally induced $Foxp3^+$ T regulatory cells. *J. Immunol.* **184,** 3433–3441 (2010).
8. Yadav, M. *et al.* Neuropilin-1 distinguishes natural and inducible regulatory T cells among regulatory T cell subsets *in vivo*. *J. Exp. Med.* **209,** 1713–1722 (2012).
9. Weiss, J. M. *et al.* Neuropilin 1 is expressed on thymus-derived natural regulatory T cells, but not mucosa-generated induced $Foxp3^+$ T reg cells. *J. Exp. Med.* **209,** 1723–1742 (2012).
10. Annison, G., Illman, R. J. & Topping, D. L. Acetylated, propionylated or butyrylated starches raise large bowel short-chain fatty acids preferentially when fed to rats. *J. Nutr.* **133,** 3523–3528 (2003).
11. Rubtsov, Y. P. *et al.* Regulatory T cell-derived interleukin-10 limits inflammation at environmental interfaces. *Immunity* **28,** 546–558 (2008).
12. Rakoff-Nahoum, S., Paglino, J., Eslami-Varzaneh, F., Edberg, S. & Medzhitov, R. Recognition of commensal microflora by Toll-like receptors is required for intestinal homeostasis. *Cell* **118,** 229–241 (2004).
13. Mazmanian, S. K., Round, J. L. & Kasper, D. L. A microbial symbiosis factor prevents intestinal inflammatory disease. *Nature* **453,** 620–625 (2008).
14. Candido, E. P., Reeves, R. & Davie, J. R. Sodium butyrate inhibits histone deacetylation in cultured cells. *Cell* **14,** 105–113 (1978).
15. Davie, J. R. Inhibition of histone deacetylase activity by butyrate. *J. Nutr.* **133,** 2485S–2493S (2003).
16. de Zoeten, E. F., Wang, L., Sai, H., Dillmann, W. H. & Hancock, W. W. Inhibition of HDAC9 increases T regulatory cell function and prevents colitis in mice. *Gastroenterology* **138,** 583–594 (2010).
17. Tao, R. *et al.* Deacetylase inhibition promotes the generation and function of regulatory T cells. *Nature Med.* **13,** 1299–1307 (2007).
18. Josefowicz, S. Z., Lu, L.-F. & Rudensky, A. Y. Regulatory T cells: mechanisms of differentiation and function. *Annu. Rev. Immunol.* **30,** 531–564 (2012).
19. Zheng, Y. *et al.* Role of conserved non-coding DNA elements in the *Foxp3* gene in regulatory T-cell fate. *Nature* **463,** 808–812 (2010).
20. Ruan, Q. *et al.* Development of $Foxp3^+$ regulatory T cells is driven by the c-Rel enhanceosome. *Immunity* **31,** 932–940 (2009).
21. Powrie, F., Leach, M. W. M., Mauze, S. S., Caddle, L. B. L. & Coffman, R. L. R. Phenotypically distinct subsets of $CD4^+$ T cells induce or protect from chronic intestinal inflammation in C. B-17 *scid* mice. *Int. Immunol.* **5,** 1461–1471 (1993).
22. Maslowski, K. M. *et al.* Regulation of inflammatory responses by gut microbiota and chemoattractant receptor GPR43. *Nature* **461,** 1282–1286 (2009).
23. Brown, A. J. *et al.* The orphan G protein-coupled receptors GPR41 and GPR43 are activated by propionate and other short chain carboxylic acids. *J. Biol. Chem.* **278,** 11312–11319 (2003).
24. Inan, M. S. *et al.* The luminal short-chain fatty acid butyrate modulates NF-κB activity in a human colonic epithelial cell line. *Gastroenterology* **118,** 724–734 (2000).
25. Thibault, R. *et al.* Down-regulation of the monocarboxylate transporter 1 is involved in butyrate deficiency during intestinal inflammation. *Gastroenterology* **133,** 1916–1927 (2007).
26. Frank, D. N. *et al.* Molecular-phylogenetic characterization of microbial community imbalances in human inflammatory bowel diseases. *Proc. Natl Acad. Sci. USA* **104,** 13780–13785 (2007).
27. Scheppach, W. *et al.* Effect of butyrate enemas on the colonic mucosa in distal ulcerative colitis. *Gastroenterology* **103,** 51–56 (1992).
28. Harig, J. M., Soergel, K. H., Komorowski, R. A. & Wood, C. M. Treatment of diversion colitis with short-chain-fatty acid irrigation. *N. Engl. J. Med.* **320,** 23–28 (1989).
29. Miyao, T. *et al.* Plasticity of $Foxp3^+$ T cells reflects promiscuous Foxp3 expression in conventional T cells but not reprogramming of regulatory T cells. *Immunity* **36,** 262–275 (2012).

Supplementary Information is available in the online version of the paper.

Acknowledgements We would like to thank P. Carninci, Y. Shinkai and M. Yoshida for discussion; Y. Chiba and S. Yamada for technical support; H. Sugahara for technical advice; and P. D. Burrows for critical reading and editing of the manuscript. This work was supported in part by grants from Japanese Ministry of Education, Culture, Sports, Science and Technology (24117524 to S.F.; 21022049 to K.Ha.; 20113003 to H.O.), The Japan Society for the Promotion of Science (24890293 to Y.F.; 252667 to Y.O.;

24380072 and 24658129 to S.F.; 22689017 to K.Ha.; 21390155 to H.O.), The Japan Science and Technology Agency (K.Ha., K.A. and K.Ho.), RIKEN President's Special Research Grant (H.O.), RIKEN RCAI Young Chief Investigator program (K.Ha.), the Institute for Fermentation, Osaka (S.F.), the Mishima Kaiun Memorial Foundation (S.F.), The Takeda Science Foundation (S.F. and H.O.), The Mitsubishi Foundation (H.O.), and The Uehara Memorial Foundation (S.F. and K.Ha.).

Author Contributions S.F., K.Ha., D.L.T., T.M., K.Ho. and H.O. conceived the study; K.Ha. and S.F. designed the experiments and wrote the manuscript with Y.Fur., Y.O. and H.O.; Y. Fur. and Y.O conducted a large part of experiments together with S.F., G.N., D.T., C.U., K.K., T.K., M.Ta., E.M. and K.Ha; S.F, S.O. and K.Ha. prepared germ-free, CRB-associated and gnotobiotic mice. K.A. and K.Ho. were involved in data discussion. S.F., Y.N., C.U. and J.K. performed metabolome analysis. S.F., T.K., S.M. and M.To. performed microbiome analysis. T.A.E. performed bioinformatic analyses. S.Hi. and T.M. performed HPLC analysis. S.F. and N.N.F. performed GC–MS analysis. Y.Fuj. performed histological analysis. T.L., J.M.C., D.L.T. and S.Ho. provided essential materials and contributed to the design of experiments. Y.Fur. and H.K. contributed to the ChIP assay. H.O. directed the study and took primary responsibility for editing the manuscript.

Author Information The microarray and ChIP-seq analysis data have been deposited at the Gene Expression Omnibus (GEO) under accession number GSE49655. The microbiome analysis data have been deposited at the DDBJ database (http://getentry.ddbj.nig.ac.jp/) under accession number DRA001105. Reprints and permissions information is available at www.nature.com/reprints. The authors declare no competing financial interests. Readers are welcome to comment on the online version of the paper. Correspondence and requests for materials should be addressed to H.O. (ohno@rcai.riken.jp), K.Ha. (hase@ims.u-tokyo.ac.jp) or S.F. (sfukuda@sfc.keio.ac.jp).

METHODS

Animals. Germ-free IQI mice were housed in germ-free isolators in the animal facility of RIKEN. Eight-to-ten-week-old male or female germ-free mice were orally inoculated with 3% (v/v) chloroform-treated murine faecal suspension (CRB)[6]. Germ-free and CRB-associated mice, which were housed in different isolators, were randomly grouped, and each group was fed with a γ-ray-sterilized CMF chow (Oriental Yeast) as a HFD, or AIN93G-fomula diet (Oriental Yeast) as a LFD for 4 weeks. To generate *B.-thetaiotaomicron*-associated mice, male or female germ-free mice of 8–16 weeks of age were colonized with a single gavage of 10^8 colony-forming units of *B. thetaiotaomicron*, JCM 5827T (Japan Collection of Microorganisms). Ten days after the inoculation, *B.-thetaiotaomicron*-associated mice were randomly grouped and each group was fed with the diet containing 15% (w/w) HAMS and HAMSB as a substitute for corn starch for 4 weeks. C57BL/6 mice and *Myd88*$^{-/-}$ *Ticam1*$^{-/-}$ mice were purchased from CLEA Japan and Oriental Bioservice, respectively. Mice were fed with AIN93G as a control diet for a week, and subsequently a diet containing 15% (w/w) HAMS, HAMSA, HAMSP or HAMSB for 4 weeks. *Foxp3-hCD2-hCD52* knock-in (*Foxp3*^{hCD2}) mice were described previously[29]. OT-II transgenic mice were from the Jackson Laboratory. All animal experiments were performed using protocols approved by Animal Studies Committees of RIKEN Yokohama Institute and Yokohama City University. Sample size was determined based on published studies using similar assays as well as the previous experience of the senior authors. No blinding was done for animal studies.

Adoptive transfer of OT-II T cells. OT-II (Ly5.2) transgenic CD4$^+$ T cells were enriched from the spleen and lymph nodes using the IMag Cell Separation System. CD3$^+$ CD4$^+$ CD25$^-$ Vα2$^+$ cells were sorted using FACSAriaII and intravenously transferred into C57BL/6 (Ly5.1) mice. Recipient mice were administered 1% ovalbumin in drinking water for 9 days.

Flow cytometry. The following monoclonal antibodies were conjugated with biotin, FITC, AlexaFluor 488, phycoerythrin (PE), PerCP-Cy5.5, PE-Cy7, allophycocyanin (APC), AlexaFluor 647, Alexa700, APC-H7, eFluor450, Brilliant Violet 421 or V500 (from BD Bioscience, eBioscience or Biolegend): anti-human CD2 (RPA-2.10), anti-mouse CD3ε (145-2C11), CD4 (GK1.5), CD25 (PC61), CD44 (IM7), CD45R/B220 (RA3-6B2), CD45RB (16A), CD62L (MEL-14), CD103 (2E7), Gr1 (RB6-8C5), folate receptor 4, FR4 (eBio12A5), Foxp3 (FJK-16 s), Helios (22F6), IL-10 (JES5-16E3) and TER119 (TER-119). Biotinylated anti-mouse/rat neuropilin-1 polyclonal antibodies were from R&D Systems.

For intracellular staining of Foxp3 and Helios, lymphocytes were pre-incubated with FcγR (CD16/CD32)-blocking monoclonal antibody (93; eBioscience) before staining for surface antigens. The cells were then fixed, permeabilized and stained with relevant monoclonal antibodies using the Foxp3 staining set (eBioscience) according to the manufacturer's instructions.

For intracellular IL-10 staining, lamina propria lymphocytes were cultured for 6 h in complete medium (RPMI1640 containing 10% FCS, 100 U ml^{-1} penicillin, 100 μg ml^{-1} streptomycin, 55 μM mercaptoethanol and 20 mM HEPES, pH 7.2) supplemented with 50 ng ml^{-1} phorbol myristate acetate, 500 ng ml^{-1} ionomycin, and Golgi Plug (BD Bioscience) in 12-well plates. The lymphocytes were then stained with monoclonal antibodies against CD3ε, CD4, CD25 and FR4, followed by intracellular staining for IL-10 using a Cytofix/Cytoperm kit (BD Bioscience). Our preliminary experiments demonstrated that the colonic CD3ε$^+$ CD4$^+$ CD25$^+$ FR4$^+$ population exclusively consists of Foxp3$^+$ cells, consistent with a previous report[30]. The stained samples were analysed using FACSCanto II and FACSAria II flow cytometers with DIVA software (BD Biosciences) and FlowJo software version 9.3.2 (Tomy Digital Biology).

Preparation of lymphocytes. Colonic lamina propria lymphocytes were prepared as described previously[31]. In brief, colonic tissues were treated with HBSS (Wako Pure Chemical industries) containing 1 mM dithiothreitol and 20 mM EDTA at 37 °C for 20 min to remove epithelial cells. The tissues were then minced and dissociated with collagenase solution containing 0.5 mg ml^{-1} collagenase (Wako Pure Chemical Industries), 0.5mg ml^{-1} DNase I (Roche Diagnostics), 2% FCS, 100 U ml^{-1} penicillin, 100 μg ml^{-1} streptomycin and 12.5 mM HEPES, pH 7.2, in RPMI 1640 medium (Sigma-Aldrich) at 37 °C for 30 min to obtain single-cell suspensions. After filtering, the single-cell suspensions were washed with 2% FCS in RPMI 1640, and subjected to Percoll gradient separation. The spleen and mesenteric lymph nodes were mechanically disrupted into single-cell suspensions.

***In vivo* EdU-incorporation assay.** To detect proliferating cells *in vivo*, HAMS- or HAMSB-fed mice received intraperitoneal injection of 3 mg EdU in 200 μl PBS, followed by administration of drinking water containing 0.8 mg ml^{-1} EdU for 2 days before the analysis. EdU-incorporated cells in cLP were visualized using Click-it EdU Flow cytometry kit (Invitrogen), following the manufacturer's instructions.

Microbiological analysis. Bacterial genomic DNA was isolated as described previously with some modifications[32]. In brief, faecal samples were lyophilized by using VD-800R lyophilizer (TAITEC) for 24 h. Freeze-dried faeces were disrupted with 3.0 mm Zirconia Beads (Biomedical Science) by vigorous shaking (1,500 r.p.m. for 10 min) using Shake Master (Biomedical Science). Faecal samples (10 mg) were suspended with DNA extraction buffer containing 400 μl 10% (w/v) SDS/TE (10 mM Tris-HCl, 1 mM EDTA, pH 8.0) solution, 400 μl phenol/chloroform/isoamyl alcohol (25:24:1), and 200 μl 3 M sodium acetate. Faeces in mixture buffer were further disrupted with 0.1 mm zirconia/silica beads (BioSpec Products) by vigorous shaking (1,500 r.p.m. for 10 min) using Shake Master (Biomedical Science). After centrifugation at 15,000*g* for 30 min at room temperature, bacterial genomic DNA was purified from the faecal extracts by a phenol/chloroform/isoamyl alcohol method. Adequate amounts of bacterial genomic DNA samples were amplified by the SYBR premix Ex Taq (TAKARA BIO) with the universal primers or *Clostridiales*-specific primers for the genes encoding the bacterial 16S rRNA sequence[33]. The results were calculated as the quantity relative to the copy number detected in the faeces of conventional mice.

454-barcoded pyrosequencing of 16S rRNA genes. The V1–V2 region of the 16S rRNA gene was amplified as described elsewhere[34]. Mixed samples were prepared by pooling approximately equal amounts of PCR amplicons from each sample and subjected to 454 GS JUNIOR (Roche Applied Science) sequencing according to the manufacturer's instructions. 16S rRNA reads were analysed using QIIME(v1.6): fasta, quality files and a mapping file indicating the bar-code sequence corresponding to each sample were used as input. The QIIME pipeline takes this input information and split reads by samples according to the bar code, and classifies all 3,000 filter-passed reads of the 16S V1–V2 sequences obtained from each sample into operational taxonomic units on the basis of sequence similarity. It also performs taxonomical classification using the RDP-classifier (v2.5)[35]. The phylogenetic tree was constructed using ClustalW 2.0 (ref. 36) with 100 bootstrap iterations. The tree was visualized with iTOL[37].

NMR-based metabolomics. Faecal and caecal metabolites were extracted by gentle shaking with 100 mM potassium phosphate buffer containing 90% deuterium oxide and 1 mM sodium 2,2-dimethyl-2- silapentane-5-sulphonate as the chemical shift reference (δ = 0.0 p.p.m.), and then analysed by ^{1}H-NMR and ^{1}H, ^{13}C-NMR (refs 38, 39). PCA and orthogonal partial least squares discriminate analysis on the caecal metabolome data were run with the SIMCA-P+ software (ver 12.0, Umetrics)[40,41]. All NMR experiments were conducted using Bruker DRX-700 spectrometer equipped with a cryogenically cooled probe. The NMR spectra were processed essentially as described[42–44]. In brief, ^{1}H-NMR data were reduced by subdividing the spectra into sequential 0.04 p.p.m. designated regions between ^{1}H chemical shifts of 0.0 to 9.5 p.p.m. After exclusion of water resonance, each region was integrated and normalized to the total of all resonance integral regions. Metabolite annotations were performed using our standard database[45,46].

Mass spectrometry. Organic acid concentrations of caecal contents and colonic tissues were determined by gas chromatography–mass spectrometer (GC–MS)[47]. In brief, 10 mg caecal contents or colonic tissues were disrupted using 3 mm zirconia/silica beads (BioSpec Products) and homogenized with extraction solution containing 100 μl of internal standard (100 μM crotonic acid), 50 μl HCl and 200 μl ether. After vigorous shaking using Shakemaster neo (Bio Medical Science) at 1,500 r.p.m. for 10 min, homogenates were centrifuged at 1,000*g* for 10 min and then the top ether layer was collected and transferred into new glass vials. Aliquots (80 μl) of the ether extracts were mixed with 16 μl *N*-tert-butyldimethylsilyl-*N*-methyltrifluoroacetamide (MTBSTFA). The vials were sealed tightly, heated at 80 °C for 20 min in a water bath, and then left at room temperature for 48 h for derivatization. The derivatized samples were run through a 6890N Network GC System (Agilent Technologies) equipped with HP-5MS column (0.25 mm × 30 m × 0.25 μm) and 5973 Network Mass Selective Detector (Agilent Technologies). Pure helium (99.9999%) was used a carrier gas and delivered at a flow rate of 1.2 ml min^{-1}. The head pressure was set at 97 kPa with split 20:1. The inlet and transfer line temperatures were 250 and 260 °C, respectively. The following temperature program was used: 60 °C (3 min), 60–120 °C (5 °C per min), 120–300 °C (20 °C per min). One microlitre of each sample was injected with a run time of 30 min. Organic acid concentrations were quantified by comparing their peak areas with the standards.

HPLC analysis of faecal organic acids. Faecal and caecal organic acids were measured by the internal standard method using an HPLC equipped with Shim-pack SCR-102H column (Shimadzu) and an electroconductivity detector (CDD-6A, Shimadzu)[48].

***In vitro* cultures.** CD4$^+$ cells were enriched from the spleen and lymph nodes of C57BL/6 mice by a negative selection method with the IMag Cell Separation System (BD Bioscience) using a mixture of biotinylated monoclonal antibodies against B220, CD8α, CD11c, Gr-1 and Ter-119 and Streptavidin Particle Plus-DM (all from BD Bioscience). The enriched CD4$^+$ fraction was subjected to cell sorting with FACSAriaII to isolate CD3$^+$ CD4$^+$CD25$^-$ CD44^{lo} CD62L^{hi} naive T cells. For T_{reg} cell polarization, naive CD4$^+$ T cells (5 × 10^5 cells ml^{-1}) were stimulated with immobilized anti-CD3 monoclonal antibody (10 μg ml^{-1}) and soluble anti-CD28 monoclonal antibody (1 μg ml^{-1}) supplemented with 0.2 ng ml^{-1} TGF-β1